# Impacts of Barrier-Island Breaching On Mainland Flooding During Storm Events

Catherine Jeffries, Robert Weiss, Jennifer Irish, Kyle Mandli

May 3, 2023

**Abstract**

Barrier islands can protect the mainland from flooding during storms by affecting the storm surge. However, the protective capability is reduced when barrier islands breach and a direct hydrodynamic connection between the water bodies on both sides of the barrier island is established. Breaching of barrier islands during large storm events is complicated, involving sediment transport and nonlinear processes that connect water and sediment transport, dune height, and island width among other factors. Because of the many factors involved in the breaching process it is difficult to predict where and when a breach will form. In order to assess how barrier-island breaching impacts flooding on the mainland, we use a statistical approach to analyze the sensitivity of mainland storm-surge runup to barrier island breaching by randomizing the location, time, and extent of a breach event. The shape of the breach is approximated with a gaussian distribution imposed on the barrier island that deepens over time. Breach formation is time dependent after a triggering event, for preliminary work specified as one meter of flow depth over the barrier island, during a simulated storm event using GeoClaw, and breach growth is limited by the flow conditions in its rate of change and when it achieves equilibrium. Varying the timing, extent, and locations

of the barrier island breaches during a storm event will provide insight into how the mainland coastline responds to breaches during storms. This insight is invaluable in preparing shoreline communities to be aware of the differing ways the regions can change during storms, depending on how the barrier islands behave. Additionally, we can offer statistical insights into where a breach would impact the mainland coastline more drastically in an effort to provide data for planning and warning purposes.

# 1 Introduction

Barrier islands are elongate, shore-parallel, low-relief land masses that are adjacent to approximately 6.5% of the world's coastlines (Oertel, 1985; Stutz and Pilkey, 2001). Oertel (1985) defines barrier island systems as containing six sedimentary environments; proximity to the mainland, a back-barrier region (bay or lagoon), an inlet and inlet delta, the barrier island, the barrier platform, and the shoreface. Barrier islands are protective structures that assist with dissipating the wave energy approaching the mainland from the ocean. The dissipation of wave energy ensures that barrier islands undergo significant change during storms and hurricanes, one of which is breaching. A breach is an opening in a narrow landmass, such as a barrier island, that allows a direct hydrodynamic connection between the ocean and the back-barrier bay or lagoon (Kraus, 2003; Kraus and Wamsley, 2003; Wamsley and Kraus, 2005; Kraus and Hayashi, 2005). Breaching that occurs naturally is a complicated process that combines waves, overwash, barrier island width and height, and storm forcing to initiate.

Large storms, such as hurricanes, can have a devastating impact on barrier islands and the mainland coastline. One of the many hazards presented by such storms is storm surge, a forced wave driven by wind and atmospheric pressure changes during the hurricane. Storm surge that causes a water level gradient between the ocean and back-barrier region will force water to flow rapidly over the barrier island and erode the sediment of the island in an effort to equalize the water level. This gradient involves a critical elevation of water levels that may not necessarily involve inundation of the island, but can still cause erosion (Kraus et al., 2002; Kraus, 2003). Storm surge and wave setup both increase the elevation of the water in the ocean and the back-barrier region; these water levels in addition to wave action reduce the stability of the barrier island dune slope (Kraus, 2003; Kraus et al., 2002). However, wave attack by itself, while weakening the dune slope, is un-

likely to induce breaching because the net erosion is seaward and does not push erosion landward (Pierce, 1970). Breaching can occur through two different transport methods, overtopping (overwash) and seepage and liquefaction (Kraus et al., 2002; Kraus, 2003).

During storm-induced overwash and inundation of the islands, the water flowing across the island can scour a channel between the sea and the back-barrier region (Kraus, 2003; Pierce, 1970; Roelvink et al., 2009). For this scouring to occur a strong flow and some duration of inundation are required. Breaching can occur from both the seaward and landward side of the barrier island but field data is limited in its ability to illustrate from which direction a breach is initiated (Kraus, 2003; Pierce, 1970; Smallegan and Irish, 2017). However, Smallegan and Irish (2017) show that bay surge that comes after peak ocean surge is more likely to lead to breaching from the landward side of the barrier island. This is due to peak ocean surge having already weakened the dune through erosion caused by wave attack and swash (Kraus, 2003; Smallegan and Irish, 2017). Breach location is challenging to correctly identify; localized lows in dune height and narrower portions of the barrier island are more likely to be potential breach locations (Kraus, 2003; Kraus and Wamsley, 2003). van der Lugt et al. (2019) simulated Hurricane Sandy (2012) with both wave forcing and sediment transport to illustrate barrier island morphodynamics during the hurricane and correctly modeled a breach but the location was simulated to be some distance away from where the breach was located in reality.

Breach dimensions are difficult to quantify, the growth of breaches over time has been documented (Kraus and Wamsley, 2003; Schmeltz et al., 1983). However, these studies address the days, weeks, or months following the storm. Initial breach size during a storm is less known. Lab and field experiments by Visser (1999) for breaches in dikes are useful but the breach is initiated with a pre-drilled hole in the dike and does not simulate exactly what occurs to barrier islands during storms. Buynevich (2006) performed a geologic mapping of some New England barrier islands and found geoloci signatures to indicate

the islands' past history with breaching and overwash. They found ephemeral breaches with widths of 10 - 30 m before closing and breach depths of one - three meters below the dune crest. A few post-storm surveys have defined breach sizes before natural or forced closing. Kraus and Wamsley (2003) discusses Pike's inlet on Long Island, NY was initially 304.8 m wide and a nearby breach named Little Pike's inlet was initially 30.48 m wide but over several months grew to over 914.4 m before it was closed. A breach near Moriches Inlet studied by Schmeltz et al. (1983) has an initial size of 91.4 m and 0.61 m depth. This breach expanded to 885 m with a three m depth before it was closed by the US Army Corps of Engineers (USACE). The uncertainties in breach dimensions and in where, how, and when breaches occur remains one of the many issues facing coastal communities today.

Barrier islands exist along the coasts of 18 states that border the Atlantic Ocean and Gulf of Mexico (Zhang and Leatherman, 2011). As coastal populations have increased considerably over the last few decades, the protective nature of barrier islands have become even more important (Zhang and Leatherman, 2011). The National Hurricane Center (NHC) states that storm surge is the largest contributor to life loss and property damage during hurricanes (National Hurricane Center, 2006). During a hurricane, storm surge induces flooding that can damage structures, close roads, and impact the lives of humans living in the coastal zone. Storm surge can also speed up erosion on both barrier islands and the mainland coast, which then can drive more flooding. Understanding how barrier island breaching affects coastal flooding from storm surge is important for risk assessment and mitigation efforts. The opening of a hydrodynamic connection between the ocean and the back-barrier region can lead to increased flooding and waves during hurricanes that increases the risk to populations and property. However, there is little information currently available on how different breach morphodynamics affect the mainland.

In this paper, we explore a method of simulatingx barrier island breach in order to evaluate the impacts of storm surge induced breaching on mainland flooding. Using a storm modeling software, GeoClaw, we artificially alter the bathymetry of a barrier island to create a breach. This process provides a more controlled method of simulating breaching than using a sediment transport model. We remove the complexities involved in the sediment transport in order to purely study the mainland's flood response to a breach opening in random locations along the barrier island and at different times during the storm simulation.

# *2 Methods*

## *GeoClaw*

Our goal for this project is to quantify the differences in coastal and bay flooding if breaching occurs during a hurricane. To simulate the storm we are running simulations with GeoClaw a subsidiary of Clawpack, a suite of conservation law programs that solve hyperbolic differential equations in one and two dimensions to model geophysical events (Clawpack Development Team, 2020; Mandli et al., 2016). Clawpack employs adaptive mesh refinement (AMR) that allows for increasing resolution where and when it is needed and reduces the computational overhead while providing an accurate solution (Berger et al., 2011). GeoClaw has been validated by the US National Tsunami Hazard Mitigation Program (NTHMP) for tsunami modeling. /citepgonzalezvalidation Describes the benchmarking process used to validate the GeoClaw.

Storm surge modeling with GeoClaw has not been validated but has been proposed to provide a robust but less computationally expensive model than ADCIRC, a commonly utilized finite element model. GeoClaw calculates storm surge with a two dimensional depth averaged model that solves the classical shallow water equations with source terms

for bathymetry, bottom friction, Coriolis forcing, surface pressure, and wind friction (Mandli and Dawson, 2014).

## *Breaching*

Breaching is a complex process that is difficult to accurately model, the storm forcing, width of the island, sediment transport, and other complex processes are all involved that make it difficult to predict where and when a breach will occur. There is a lack of studies which document barrier island breach dimensions, due to the nature of storm induced breaching, it is dangerous if not impossible to quantify what exactly occurs to create a breach in a barrier island during a hurricane. Lab studies of breaches in dikes provides some clues into breach formation (Visser, 1999). Studies that map out breaches usually occur well after the storm which aren't accurate to initial breach width and depth as breaches will continue to grow as water passes between the ocean and back-barrier region.

To accomplish our goal of quantifying flooding due to breaching we chose to simplify breaching by reducing the topography of the barrier island at specific locations. We simulate a breach using an approximation of a gaussian function to provide a breach with sloping sides and the deepest part in the center. During the storm simulation we apply 1 to reduce the height of the barrier island at a selected location, where $\mu$ is the center of the breach location, $d^t$ is the height of the breach location at time *t*, *X* is the longitude of the location being reduced and $t_T$ is a timing factor that controls how quickly the breach opens. The timing factor for these simulations allow for the breach to open fully in an hour after Visser (1999).

$$d^t = d^{t-1} - e^{-\frac{1}{2}(X-\mu)^2} t_T \tag{1}$$

## *Storm Forcing*

The storm we employ to simulate storm surge is a proxy for the 1938 New England hurricane. The storm data was generated for the US Army Corps of Engineers (USACE) North Atlantic Comprehensive Coast Survey (NACCS) (Cialone et al., 2015). The storm forcing is provided by wind and pressure fields that have data in 15 minute increments. Accurate modeling of this storm requires sub-minute data and AMR requires data to be integrated at increasing resolution where needed. To provide the sub-minute time steps we use linear interpolation of the wind and pressure fields, to define the wind and pressure forcing inside the AMR grids we employ bi-linear interpolation when and where it is required. The chosen storm has a similar track and intensity of the 1938 hurricane. We can verify the accuracy of the solution with a tide gauge at Sandy Hook, NJ that has data recorded from 1938, once adjustments are made for modern bathymetry and sea levels.

## *1938 Hurricane*

The 1938 hurricane at Moriches, NY caused six breaches, three west of the inlet and three east of the inlet; quantifying the bay and coastal flooding changes during this hurricane requires that we vary the locations, timing, width, and depth of these breaches and recording the differences in synthetic tide gauges placed around the bay and recording maximum water levels in a large grid that is resolved to 18 meters. A no breach scenario provided the baselines we used for quantifying differences in breaching scenarios and verifying a breaching location is viable. We simulated synthetic tide gauges on the seaward side of the bay as a proxy for island inundation. Once a breach location is chosen we verify it is viable by taking the synthetic tide gauges within one km of the breach and calculate that the tide gauge reaches a minimum of 24% of the dune height. If no gauges within one km reach that water height we choose a new location and start the test over.

This allows for a reasonable estimate of the conditions that could induce breaching, if the water levels just offshore do not reach a critical height it is unlikely a breach would open at that location.

## *Simulations*

Our simulations were set up with with a basin scale bathymetry using GEBCO 30 arc second (Weatherall et al., 2015) for the region that spans 98W to 57 W and 5N to 45N. Moriches, NY bathymetry is from NOAA's continuously updated 1/9 arc second topobathy dataset (for Research in Environmental Sciences), 2014). Use modifed GeoClaw's AMR to focus on the bay at 18 x 18 meter cells that is refined well before the storm arrives to observe the surge as it enters the bay. We place synthetic tide gauges dispersed through the bay in the same configuration that was used for the NACCS project maximum surge locations (**?**) and a series of tide gauges on the seaward side of the barrier every two kilometers that we used to verify offshore surge height for breach initiation.

We started with the original six breach dimensions as estimated from Cañizares and Irish (2008), from there we created a monte-carlo framework that employs a random uniform distribution for each breach's size and location. The time of initiation for each breach was chosen using the nearest synthetic tide gauge data from a no breach simulation; the first time in seconds the nearest tide gauge reaches 24% of the maximum dune height at each location was our start time. We chose to have the breaches fully open within one hour after initiation.

For our first grouping of scenarios we used the original breach locations formed during 1938 Hurricane. Our first set of simulations we held the depth steady at -2.0 meters and varied the widths for each breach individually between 25 - 630 meters which is the largest size of the breaches formed during the 1938 hurricane. Our second set of scenarios, we kept the original 1938 breach width estimations and varied the depths between 0 and -2.0

meters. The endpoints for each randomization was chosen from examples in the literature (Schmeltz et al., 1983; Kraus and Wamsley, 2003; Visser, 1999; Cañizares and Irish, 2008). We then randomized both the breach width and depth and number of breaches with a maximum of six breaches. Finally, we varied; the number of breaches, the width, the depth, and the locations of each breach. We used a maximum number of breaches as the maximum 'viable' locations per our criteria above. This provided a maximum of 295 individual breach locations possible.

### *2.1 Data analysis*

We evaluated our results using the maximum surge height data recorded by GeoClaw for the entire bay and at select synthetic tide gauges. We divided the bay into three sections, west, central, and east, we compared the different types of simulations. We calculated inundation differences by first identifying the grid cells that were on land in the bathymetry, and were inundated in a no breach scneario (wet cells). We used that grid of cells to then identify the changes in inundation for each simulation. Each cell is an 18x18 square meters which provides a total area of 324 square meters. Comparing this against the no breach scenario provides us insight into how different breach dimensions affect the total inundation area of the region. Additionally, We gathered the data from our select bay tide gauges and calculated the mean of each category of simulation to visualize trends in the different categories across the surge timing and locations.

## *3 Results*

To analyse the results we looked at both surge height at random points in the bay and total inundation in square meters. Figure 1 illustrates the locations of each chosen storm surge point and the locations of the synthetic tide gauges for each section of the bay.

[Figure 1 about here.]

We chose three random locations by first dividing the bay into thirds, and for each section (west, central, east) we used a random uniform distribution to choose the point to study the maximum surge. Figure 2 illustrates the surge heights for each category of simulation. The mean of the surge height is higher for the random everything variations with the density peak at 1.75, 1.70, 1.43 for west, central, east bay respectively. The variance is also large at 0.05, 0.024, 0.03 as compared to the other simulations. When constrained by a maximum of six breaches the depth variations have the largest surge height mean at 1.06, 1.07, .84. The width scenarios mean surge height is 0.97, 1.09, 0.78 and the width/depth/number of breaches simulations have a mean surge height of 0.88, 0.98, 0.72. The width scenarios have a larger variance of 0.004, 0.004, 0.002 as compared to depth 0.003, 0.0003, 0.005 or both 0.006, 0.002, 0.002.

[Figure 2 about here.]

Figures 4. illustrate that different inundation patterns are correlated to number and size of breaches. Figure 4a is a no breach scenario which looks very similar in surge and inundation distribution to the minimum inundation which has only a single small breach. There are only approximately 500 different wet vs. dry cells between these two, which is 163,000 square meters or .1632 square kilometers of inundation. The scenario that comes closest to the mean of all the inundation is six moderately sized breaches with an area of .005 $km^2$ and total inundation change of 13.06 $km^2$ the pattern of bay flooding and inundation is very different from the no breach or minimum inundation scenarios, with higher flooding potential in the river drainages and along the lower elevation coastlines. Lastly the maximum inundation scenario is one where most of the island has been inundated, this scenario has a bay surge of approximately 2 meters in most areas and the lowest elevation areas of the coastline completely flooded.

# 4 Discussion

[Figure 3 about here.]

Figure 3 illustrates that total breach area in the island is the strongest determining factor in higher mainland inundation. The depth variations show a higher mean inundation area due to some of the original breaches being very large, on the order to 20-100 times wider than the total depth. Single small breaches have less inundation potential than multiple small breaches or many breaches of mixed total area. Total width runs from 25 - 630 meters whereas total depth goes from 0 to -2.0 meters. Changing the locations of the breaches adn varying the number of breaches allowed to be the total number of viable sites on the island (around 295) shows...

# 5 Conclusions

Breaching of a barrier island during a hurricane shows a strong impact on mainland inundation. The number/(location?)/ and size of the breaches can change the inundation potential.

Future work: Run many (1000s) more simulations to be able to get a full distribution of data from depth/width breaching differences. Run more storms to show impacts from different approaches, storm sizes, storm structure (extratropical like Sandy?), storm speeds to perform the same analysis and gain a better understanding of breaching impacts. Do storms

# References


M. J. Berger, D. L. George, R. J. LeVeque, and K. T. Mandli. The GeoClaw software for depth-averaged flows with adaptive refinement. *Advances in Water Resources*, 34 (9):1195–1206, 9 2011. ISSN 03091708. doi: 10.1016/j.advwatres.2011.02.016. URL http://linkinghub.elsevier.com/retrieve/pii/S0309170811000480 file:///Users/kitty/Library/Mobile Documents/com apple CloudDocs/Papers/Papers Library/Files/69/69E24870-C44F-49FD-BB3E-73EF76EEBE02.pdf papers3://publication/doi/10.1016/j.advwatres.2011.02.01.

I. V. Buynevich. Geological signatures of barrier breaching and overwash. *Journal of Coastal Research*, 2004(39):112–116, 2006. ISSN <null>.

R. Cañizares and J. L. Irish. Simulation of storm-induced barrier island morphodynamics and flooding. *Coastal Engineering*, 55(12):1089–1101, 2008. ISSN 03783839. doi: 10.1016/j.coastaleng.2008.04.006. URL http://dx.doi.org/10.1016/j.coastaleng.2008.04.006.

M. A. Cialone, T. C. Massey, M. E. Anderson, A. S. Grzegorzewski, R. E. Jensen, A. Cialone, D. J. Mark, K. C. Pevey, B. L. Gunkel, and T. O. McAlpin. North atlantic coast comprehensive study (naccs) coastal storm model simulations: Waves and water levels. Technical report, ENGINEER RESEARCH AND DEVELOPMENT CENTER VICKSBURG MS COASTAL AND HYDRAULICS LAB, 2015.

Clawpack Development Team. Clawpack software, 2020. URL http://www.clawpack.org. Version 5.7.1.

C. C. I. for Research in Environmental Sciences). Continuously updated digital elevation model (cudem)—1/9 arc-second resolution bathymetric-topographic tiles, 2014.

N. C. Kraus. Analytical model of incipient breaching of coastal barriers. *Coastal engineering journal*, 45(04):511–531, 2003. ISSN 0578-5634. doi: 10.1007/978-94-017-8801-4_279.

N. C. Kraus and K. Hayashi. Numerical Morphologic Model of Barrier Island Breaching. In *Coastal Engineering 2004*, pages 2120–2132. 2005. doi: 10.1142/9789812701916_0170.

N. C. Kraus and T. V. Wamsley. Coastal Barrier Breaching , Part 1 : Overview of Breaching Processes. *US Army Corps of Engineers*, (March):1–14, 2003.

N. C. Kraus, A. Militello, and G. Todoroff. Barrier Breaching Processes and Barrier Spit Breach, Stone Lagoon, California. *Shore & Beach*, 70(4), 2002. ISSN 00045772.

K. T. Mandli and C. N. Dawson. Adaptive mesh refinement for storm surge. *Ocean Modelling*, 75:36–50, 2014. ISSN 14635003. doi: 10.1016/j.ocemod.2014.01.002.

K. T. Mandli, A. J. Ahmadia, M. Berger, D. Calhoun, D. L. George, Y. Hadjimichael, D. I. Ketcheson, G. I. Lemoine, and R. J. LeVeque. Clawpack: building an open source ecosystem for solving hyperbolic pdes. *PeerJ Computer Science*, 2:e68, 2016.

National Hurricane Center. Hurricane Preparedness - Hazards, 2006. URL `https://www.nhc.noaa.gov/prepare/hazards.php`.

G. F. Oertel. The barrier island system. *Marine Geology*, 63(1-4):1–18, 1985. ISSN 00253227. doi: 10.1016/0025-3227(85)90077-5.

J. Pierce. Tidal Inlets and Washover Fans Author. *The Journal of Geology*, 78(2):230–234, 1970. URL `http://www.jstor.org/stable/30063791`.

D. Roelvink, A. Reniers, A. Van Dongeren, J. Van Thiel De Vries, J. Lescinski, and R. McCall. Modeling storm impacts on beaches, dunes and barrier

islands. *Proceedings of the Coastal Engineering Conference*, 56(11-12):1684–1696, 2009. ISSN 01613782. doi: 10.1016/j.coastaleng.2009.08.006. URL http://dx.doi.org/10.1016/j.coastaleng.2009.08.006.

E. J. Schmeltz, R. M. Sorensen, M. J. McCarthy, and G. Nersesian. Breach/Inlet Interaction At Moriches Inlet. *Proceedings of the Coastal Engineering Conference*, 2: 1062–1077, 1983. ISSN 0589-087X. doi: 10.9753/icce.v18.66.

S. M. Smallegan and J. L. Irish. Barrier island morphological change by bay-side storm surge. *Journal of Waterway, Port, Coastal and Ocean Engineering*, 143(5):1–10, 2017. ISSN 0733950X. doi: 10.1061/(ASCE)WW.1943-5460.0000413.

M. L. Stutz and O. H. Pilkey. A review of global barrier island distribution. *Journal of Coastal Research*, (Special Issue 34):15–22, 2001. doi: 10.2307/25736270. URL http://www.jstor.org/stable/25736270.

M. A. van der Lugt, E. Quataert, A. van Dongeren, M. van Ormondt, and C. R. Sherwood. Morphodynamic modeling of the response of two barrier islands to Atlantic hurricane forcing. *Estuarine, Coastal and Shelf Science*, 229(May): 106404, 2019. ISSN 02727714. doi: 10.1016/j.ecss.2019.106404. URL https://doi.org/10.1016/j.ecss.2019.106404.

P. J. Visser. Breach erosion in sand-dikes. In *Coastal Engineering 1998*, pages 3516–3528. 1999.

T. V. Wamsley and N. C. Kraus. Coastal Barrier Island Breaching, Part 2: Mechanical Breaching and Breach Closure. *Erdc/Chl Chetn-Iv-65*, (August):21, 2005.

P. Weatherall, K. M. Marks, M. Jakobsson, T. Schmitt, S. Tani, J. E. Arndt, M. Rovere, D. Chayes, V. Ferrini, and R. Wigley. A new digital bathymetric model of the world's oceans. *Earth and space Science*, 2(8):331–345, 2015.

310 K. Zhang and S. Leatherman. Barrier Island Population along the U.S. Atlantic and
311 Gulf Coasts. *Journal of Coastal Research*, 27(2):356, 2011. ISSN 1551-5036. doi:
312 10.2112/jcoastres-d-10-00126.1.

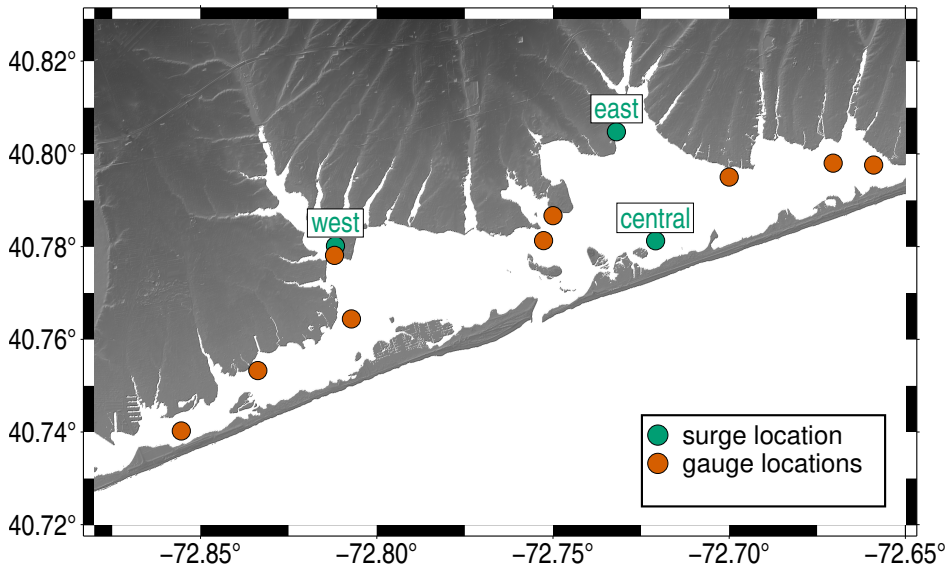


Figure 1: Map of Moriches Bay, NY. Orange circles indicate locations of synthetic tide gauges. Teal circles indicate locations of surge data

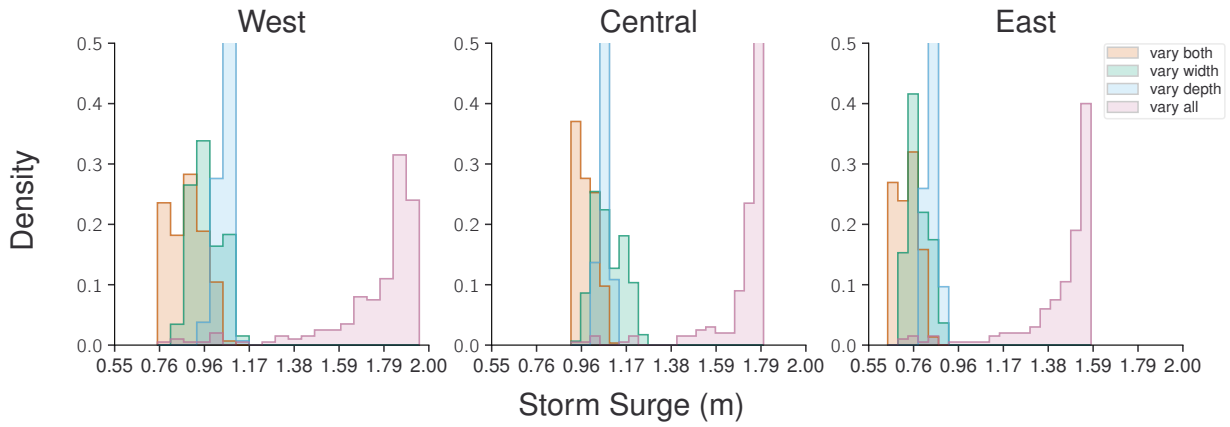


Figure 2: Maximum surge height in meters for each selected location shown in Figure 1 (green dots). Data shows 1500 scenarios split into four categories. Six breaches where width is randomized (blue) (464 scenarios), six breaches where depth is randomized (green) (424 scenarios). Varying width, depth, and number of breaches up to six breaches (orange) (297 scenarios). Varying width, depth, location, and number of breaches up to 295 breaches (315)

Figure 3a illustrates the relationship between total breach area ($km^2$) and total inundation change from a no breach simulation. The relationship starts with a minimum inundation of .1632 $km^2$ and illustrates that more breach area leads to more inundation to a point, around 75 possible breaches the curve levels off at a total breach area of .035 $km^2$ and an inundation change around 40.1 square kilometers. Inundation change grows more slowly beyond this point to a maximum total inundation of 49.06 $km^2$. Figure 3b zooms in on an the initial curve of simualations with under 20 breaches.

Figure 4 shows the differences between two simulations with the a similar total breach area, however the total inundation is very different. Figure 4a, shows a scenario with six breaches in the locations that occurred during the 1938 hurricane, the total breach area is .0039 $km^2$, and total inundation is 10.44 $km^2$. Figure 4b, has a smaller breach area at .0036 $km^2$ but a larger inundation at 12.03 $km^2$.

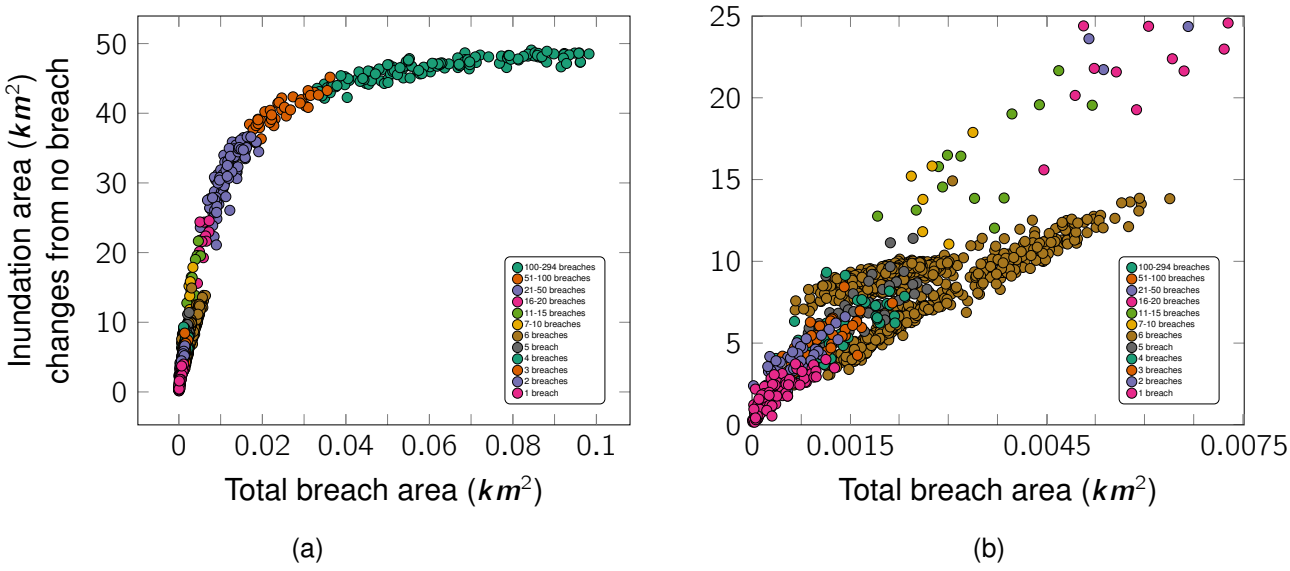


Figure 3: a) Total inundation vs. total breach size for all 1500 scenarios, points are colored per number of breach categories. b) zoom in of a) panel to show differentiation of breach area and number of breaches and how the inundation can vary

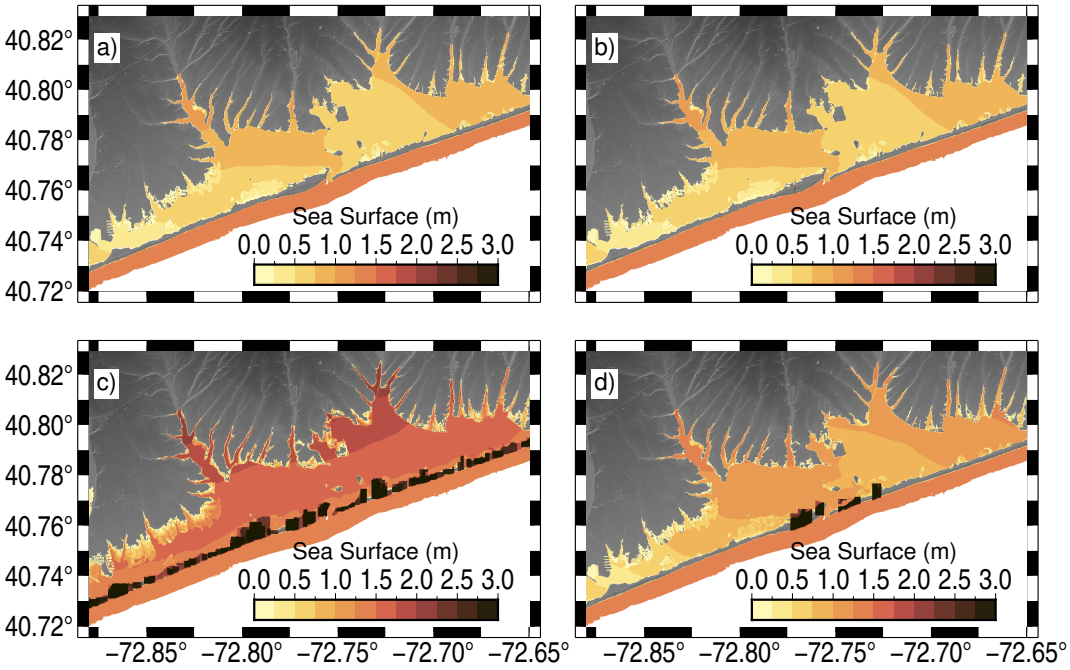


Figure 4: Maps Moriches Bay, NY. Each panel is a separate simulation representing different values of storm surge inundation. Panel (a) is no breach scenario. Panel (b) is the minimum inundation with a single small breach. Panel (c) is the largest inundation scenario with 6 wide breaches. Panel (d) is a simualation that has the closest inundation to the mean of all 1500 simulations, with 4 moderate sized breaches.

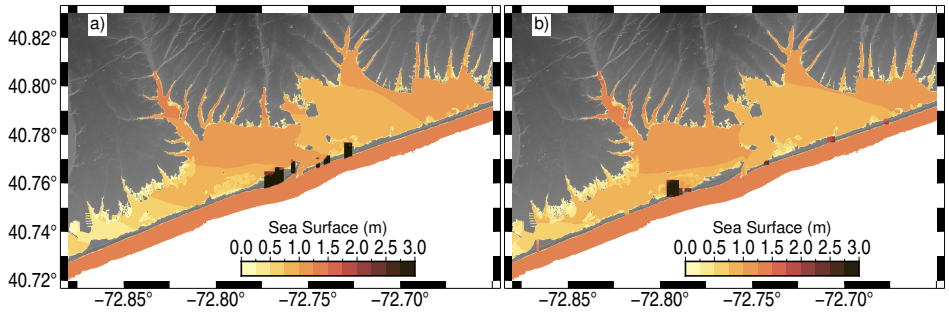


Figure 5: a) maximum surge and inundation for simulation that has 11 breaches and a total area of .036 $km^2$. b) maximum surge and inundation for simulations with 6 breaches and .039 $km^2$